Ink-Eliminated Waste Paper Sludge Flour-Filled Polypropylene Composites with Different Coupling Agent Treatments

Xiuying Qiao, Yong Zhang, Yinxi Zhang, Yutang Zhu

Research Institute of Polymeric Materials, Shanghai Jiaotong University, Shanghai 200240, People's Republic of China

Received 6 June 2002; accepted 19 September 2002

ABSTRACT: Ink-eliminated sludge flour (IESF), waste residue from the recycling treatments of waste paper, was utilized as a new kind of filler to reinforce polypropylene (PP) in this research work. Different coupling agents, including maleated anhydride grafted PP (MAPP), stearic acid (SA), and titanate (NDZ-101), were used to increase the compatibility between IESF and PP. By using different measurements, the microstructure, morphology, thermal behaviors, and mechanical properties of the IESF/PP composites were investigated in detail. It was found that IESF, as a nucleation agent, not only induced the crystallization orientation of PP but also accelerate the crystallization rate of PP. Just as indicated in the experiments, the presence of IESF has shown the advantages of increasing the dimensional stability, the hardness and the flexural property, and the presence of coupling agents has a favorable effect on the improvement of dimensional stability. Moreover, the coupling agent has minor influence on the mechanical property, even causes some decrease in the impact strength. Among these three coupling agents, MAPP is found to be the best coupling agent for increasing the interfacial adhesion between IESF and PP, and the MAPP addition makes the PP composite possess the quickest crystallization rate and greatest tensile strength. © 2003 Wiley Periodicals, Inc. J Appl Polym Sci 89: 513–520, 2003

Key words: poly(propylene) (PP); composites; fillers; compatibility; crystallization

INTRODUCTION

During the recycling treatments of the waste paper, large amounts of ink-eliminated sludge exist in the waste residue. In the light of normally produced newspaper, the quantity of the sludge from recycling treatments could amount to 90% of the total waste residue in the ink-eliminated system. In China, statistic data reveal that merely in a middle-scale waste paper disposal industry, about 50,000 tons of such ink-eliminated sludge will be produced in 1 year. The disposal of these large quantities of ink-eliminated sludge has brought great pressure on the environment protection. Although most of the paper sludge is land filled and some of the sludge is incinerated or utilized for farming, the following disadvantages of occupying enormous land and raising the accumulation of poisonous substance are still difficult environmental problems perplexing humans. Therefore, putting the paper sludge to more rational disposal and use and further changing waste materials into things of value finally have become the research focus increasingly all over the world.[1,2]

Correspondence to: Y. Zhang (yxzhang@sjtu.edu.cn).

Journal of Applied Polymer Science, Vol. 89, 513–520 (2003)

Polypropylene (PP), as a kind of general plastic and thermoplastic polymer, has been widely used in many fields of production and life, such as package, furniture, automobile manufacture, and electrical equipment, owing to its low cost, low density, and favorable advantages of processibility, heat resistance, tensile strength, and corrosion resistance. Similar to other plastics, during the application, PP was often physically modified by filling with mica, talc, calcium carbonate, and glass fiber for lowering price and property modification. However, recently, some natural fibers, such as wood,[3–5] cellulose,[6] jute,[7] bamboo,[8,9] and conifer,[10] have attracted much attention of research people as new fillers for PP, due to their low price, low density, high stiffness, and low abrasion during processing compared with traditional mineral fillers. It is the favorable price–performance ratio that makes these renewable and biodegradable natural fibers become promising substitutes for the conventional fillers. In addition, the improvement of the interfacial bonding between the hydrophilic fiber and the hydrophobic PP has been a key research issue, because the interfacial adhesion between the filler and PP plays an important role in the determination of the composites properties. Generally, to improve the compatibility between the filler and matrix, two methods were often used. One method is the modification of the filler surface using coupling agents including silane, titanate, and other small molecular coupling agents; the

other method is the modification of the matrix by grafting some small molecules with different chemical group to polyolefin chains such as acrylic acid, maleic anhydride, and acrylic esters. In fact, maleated anhydride-grafted polypropylene (MAPP) is commonly used as a compatilizer, because it can efficiently improve the fiber–matrix bonding due to the formation of covalent linkages and hydrogen bonds between the maleated anhydride and the hydroxyl groups of the fiber.[7,11]

The ink-eliminated waste paper sludge flour (IESF), as a challenge to conventional fillers, contains not only kaolin, a fine white clay, but also some short cellulose fibers, which makes it possible to be utilized as an effective filler in the manufacture of thermoplastic polymer composites. If IESF is filled into plastics for preparing polymer composites, there will be wide commercial applications and development prospects, out of the considerations of the great advantages of further lowering cost and the property modification from both inorganic and organic fillers. Most importantly, the pressure on environmental protection can be lightened, and the idea of changing waste materials into things of value for IESF can be realized. Although much research work about the treatments and the application of paper sludge has been reported, the detailed information about the structures and properties of IESF-filled thermoplastic composites and the influence of different coupling agent treatments are seldom mentioned. In this article, four kinds of PP composites were prepared with different coupling agent treatments. As for these IESF/PP composites, the structures, properties of the composites and the influence of different coupling agent treatments were also investigated in detail.

EXPERIMENTAL

Materials

A commercial polypropylene (PP), K8303, obtained from Beijing Yanshan Petrochemical Co., Ltd. (BYPC), was chosen as the polymer matrix for the preparation of the ink-eliminated waste paper sludge flour-filled PP composites. This PP, with a density of 0.91 g/cm^3 and a melt flow index of 1.6 g/10 min (230°C, 2.16 kg), comprised ethylene–propylene block copolymer in the form of spheres with high-impact strength. Ink-eliminated waste paper sludge flour (IESF) was obtained after the treatments of the sludge from waste paper recycling mill by drying, grounding and sieving to be 80–200 mesh finally. To improve the interfacial adhension between the IESF filler and PP matrix, three different coupling agents of stearic acid (SA), titanate (NDZ-101), and maleated anhydride polypropylene (MAPP) were used for the preparation of IESF/PP composites. The SA and NDZ-101 for the surface treatments of IESF were also commercial grade products. MAPP was prepared in the lab by direct reactive melt extrusion, and the grafting rate was measured as 0.3 mol %.

The surface treatment of IESF was performed in the high-speed mixer for 15 min through mixing the IESF and the coupling agents of SA and NDZ-101 with a weight ratio of 1.0% with respect to the IESF mass. The temperatures of surface treatment were 100 and 50°C for the IESF-SA/PP and IESF-NDZ/PP composites, respectively. During the preparation of the IESF/PP composites, PP was melt blended with IESF, IESF and MAPP, surface-treated IESF by SA, and surface-treated IESF by NDZ-101 titanate, respectively, and the obtained composites were then designated as IESF/PP, IESF/PP/MAPP, IESF-SA/PP, and IESF-NDZ/PP, respectively. All the IESF/PP composites contained 30 wt % IESF, and the content of MAPP was kept at 3 wt % in the composite. These four kinds of IESF/PP composites mentioned above were prepared by the use of twin-screw extruder after physically premixing the components in an SHR-10A high-speed mixer for 15 min at room temperature. The temperatures of the five processing zones were 180, 185, 190, 195, and 195°C, respectively, the screw speed was 250 rpm, and material output was 18 kg/h. After melt blending in the twin-screw extruder, the extruded strands were cooled in a cold water bath, pulled, palletized to granules, and dried at 80°C for 3 h before injection molding. By the use of a HFT 150 screw injection-molding machine, the composite pellets were injection molded into ASTM standard specimens for mechanical measurements. The temperatures of the four injection zones were 220, 220, 210, and 200°C, respectively, and the injection pressure was 60 MPa. All the specimens were conditioned at 23°C for 48 h before testing.

As for the IESF/PP, IESF/PP/MAPP, IESF-SA/PP, and IESF-NDZ/PP blends, their melt flow indexes (MFI) were determined as 2.1, 1.9, 2.0, and 2.4 g/10 min, respectively, by a RL-11A rheometer referring to the standard of ASTM D1238-88 with a load of 2.16 kg at 230°C, and their density values were measured as 1.015, 1.050, 1.054, and 1.053 g/cm^3, respectively, according to the ASTM D792-91 standard. Thus, it can be seen that the IESF filler addition has improved the rheological behavior, especially with the introduction of the coupling agent of titanate. In addition, the incorporation of IESF filler also increased the density of the composites to a small extent, and this effect was deepened by the addition of the coupling agents.

Measurements

A Rigaku D_{max}-rC X-ray diffractometer with a CuK_α radiation was used for X-ray diffraction studies. The measurements were carried out at 40 kV and 100 mA

from 1 to 40° at a scanning rate of 10°/min with an interval of 0.02°, and the specimens for measurements were some circular slices obtained from injection molding. Moreover, the detailed structural information was achieved by the use of Perkin-Elmer Paragon 1000 Fourier Transform Infrared Spectrometer (FTIR). The specimens were thin films (about 30-μm thick) obtained from the hot pressing of the composite pellets, and the FTIR spectra were recorded from 450 to 4000 cm^{-1}. These measurements were all operated at room temperature.

The Differential Scanning Calorimeter (DSC) measurements were performed in a Perkin-Elmer PYRIS 1 DSC calibrated with indium standard at the atmosphere of nitrogen. The samples, prepared from the palletized granules, were first heated quickly from room temperature to 200°C and held there for 5 min to remove the thermal history, and cooled to room temperature at 10°C/min to record the crystallization behavior, and then reheated to 200°C at 10°C/min to trace the melting behavior. Values of crystallization and melting entropy (ΔH_c and ΔH_m) were calculated from the exothermic and endothermic peak areas, and the exothermic and endothermic peak temperatures were taken as crystallization and melting temperatures (T_c and T_m). With the use of a Perkin-Elmer TGA-7 Thermogravimetric Analyzer, the weight change of the composites was investigated from room temperature to 800°C at a heating rate of 20°C/min in a nitrogen atmosphere.

The morphology of the composites was observed with a Hitachi S-2150 Scanning Electron Microscope (SEM) operated at 20 kV. Prior to examination, the sludge flour and liquid nitrogen freeze-fractured samples from injection-molded strips were coated with a thin gold layer to increase the surface conductivity.

An Instron 4465 Universal Tensile Tester was employed to evaluate the tensile and flexural property according to the ASTM standards of D638-94b and D790-92, respectively. The crosshead speeds during the tensile and flexural measurements were 50.0 and 2.0 mm/min, respectively. During the three-point flexural testing, the support span length was kept to be 50 mm. The Izod impact strength of the notched and unnotched specimens was measured by using a Ray-Ran Universal Pendulum Impact Tester following the ASTM D256-97 standard with the hammer weight of 0.818 kg and the impact energy of 5 J. A Zwick 3106 Hardness Tester was used for measurements of the hardness of the composites according to the standard of DIN EN 2039-1. Five specimens for each sample were tested to obtain the average value for determination. The heat distortion temperatures of the composites under a compression load were studied using 2 Station HDT/Vicat Softening Point Apparatus according to the standard of ASTM D648-82, and the tested samples were injection-molded strips.

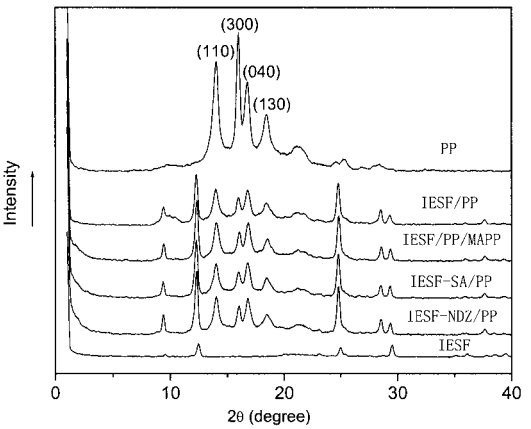

Figure 1 The X-ray diffraction patterns of the IESF/PP composites.

RESULTS AND DISCUSSION

Structure analysis

The X-ray diffraction patterns of the IESF/PP composites and the pure materials are shown in Figure 1. It can be seen in Figure 1 that the X-ray diffraction of the IESF/PP composites shows the separate characteristic diffraction peaks of iPP and IESF. Although the PP used in this study is an ethylene–propylene copolymer, the characteristic diffraction of polyethylene (PE) cannot be observed clearly because of its minor amount contained. For PP and the IESF/PP composites, the diffraction peaks located at 14.02°, 16.78°, and 18.48° should be attributed to the characteristic diffraction from the (110), (040), and (130) planes of the α-phase of iPP, while the diffraction peak at 15.98° should be attributed to the characteristic diffraction from the (300) plane of the β-phase of iPP. Generally, iPP possesses five crystal forms, such as α, β, γ, δ, and quasi-hexagonal crystal. Among those crystal forms, the α-phase, which belongs to the monoclinic system, is a common one with the best thermal stability. As can be seen in Figure 1, after the composition with IESF, the characteristic peaks of PP has almost no change in position. Nevertheless, as for the IESF/PP composites, the intensity of (040) diffraction increases to almost equal to that of (110) diffraction, and the intensity of (300) diffraction decrease greatly to less than those of (110) and (040) diffractions, which are greatly different from the diffraction pattern of pure PP in Figure 1. Thus, it can be seen that the addition of IESF not only induced the crystallization orientation of iPP along the b-axis due to its nucleation agent just as reported before,[12] but also had a restraining effect on the crystallization of the β-phase of iPP at the same time. The restraining effect mentioned above can also be demonstrated by the comparison among the K values (see Table I), which describe the relative amount of the β-phase in the crystals.[8] It should be

TABLE I
The Crystalline Phase Analysis of PP for the IESF/PP Composites

Sample	α-Phase			β-Phase	
	L_{110} (nm)	L_{040} (nm)	L_{130} (nm)	L_{300} (nm)	K-Value
PP	10.74	3.59	5.47	19.40	0.345
IESF/PP	10.74	9.72	5.18	12.90	0.229
IESF/PP/MAPP	12.87	10.78	5.47	13.81	0.230
IESF-SA/PP	11.37	11.40	8.87	12.90	0.228
IESF-NDZ/PP	12.87	11.40	5.95	13.81	0.232

noted that the addition of coupling agents has almost no influence on the positions and relative intensities of those characteristic peaks of PP in the IESF/PP composites. The effects of the IESF fillers on the formation of the crystalline phases of PP in the composites can also be described by the change of the crystallite size L_{hkl}, which represents the mean dimension of crystallites perpendicular to planes hkl and can be calculated according to the Sherrer equation.[13] The crystallite size of the crystalline phases of PP for the pure PP and IESF/PP composites are listed in Table I. From Table I, it can be clearly observed that in the presence of IESF, the crystallite sizes of (040) for the α-phase and (300) for the β-phase have a drastic increase and a dramatic decrease separately, and the coupling agent addition can lead to a little increase in the crystallite size of both the two crystalline phases of PP. Then the restriction influence of the IESF fillers and the advantageous effects of coupling agents on the crystallization of PP are obvious. Moreover, the X-ray diffraction of IESF shows its diffractions centered at 9.58°, 12.44°, 24.98°, and 29.52°, respectively, which are corresponding to the characteristic diffraction of kaolin. After the blending of IESF with PP, all these characteristic peaks obviously had a left shift in Figure 1. The resulting change of the crystalline plane spacing of IESF may be caused by the interaction of the PP molecular chains during crystallization. Meanwhile, the addition of coupling agents has minor effects on the diffractions of IESF in the composite system, and merely makes the latter three diffractions mentioned above have a little increase in intensity.

To obtain the detailed structural information and examine the bond interactions within the IESF/PP composites, FTIR experiments were performed on the composites and the pure components for comparison. Figure 2 illustrates the FTIR spectra of the IESF, PP, and the IESF/PP composites. As seen in Figure 2, PP shows its characteristic peaks at 1459 cm^{-1} from the asymmetry stretching vibration of CH_3, 1376 cm^{-1} from the symmetry bending vibration of CH_3, and 1167, 998, 973, 899, 841, and 810 cm^{-1} from the mixing vibration of the rocking of CH_3 and —CH_2 and the stretching of CH—CH_2 and CH—CH_3. However, because of the minor concentration of ethylene units in PP, the IESF/PP composites and PP have not shown the characteristic absorbance of 720 cm^{-1} for PE segments. Similar to the X-ray diffraction experiments, the IESF/PP composites illustrate separate characteristic absorbance of IESF and PP, and the absorbance peaks almost keep the same position. Although the FTIR spectra of the IESF/PP composites are similar to one another, there are also a little position difference of the absorbance peak at 1459 cm^{-1}, a little weakening and broadening of the absorbance peak at 1376 cm^{-1}, and the intensity decrease of the characteristic absorbance peaks of IESF and PP, with the coupling agent addition. Meanwhile, the effect of a coupling agent makes the stretching vibrations of —OH at 3344 cm^{-1} and absorbed water in the 1650–1600 cm^{-1} region have a little decrease in intensity, compared to those of IESF and the IESF/PP composites, which can provide an advantageous support for the interaction between the hydroxyl group in fillers and the polar group of the coupling agents.

Thermal analysis

The DSC cooling and heating scans of the IESF/PP composites are given in Figure 3, and the values of temperature and enthalpy during the crystallization and melting processes are shown in Table II. During the DSC measurements it was found that IESF had neither exothermic nor endothermic peaks in the temperature range from 50 to 200°C, thus indicating that the crystallization and melting behaviors of the

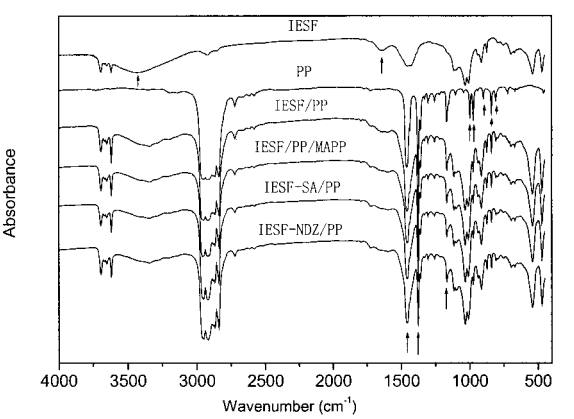

Figure 2 The FTIR spectra of the IESF/PP composites.

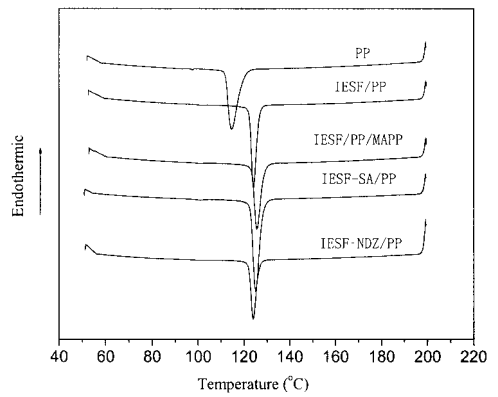

(a)

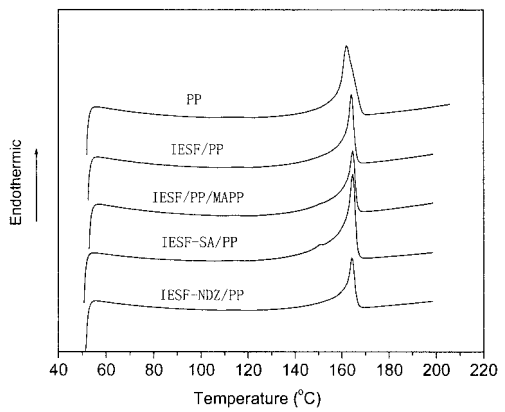

(b)

Figure 3 The cooling and heating DSC scans of the IESF/PP composites: (a) the first cooling scan; (b) the second heating scan.

IESF/PP composites in this studied temperature region are directly related to those behaviors of PP. Compared with pure PP, the IESF/PP composites possess higher crystallization and melting temperatures, lower crystallization enthalpy and heat of fusion, and narrower and sharper exothermic and endothermic peaks. Among the IESF/PP composites, the coupling agent addition of MAPP and SA has a favorable effect of increasing the crystallization and melting temperatures, while the IESF/PP/MAPP composite possesses the greatest values of temperature and enthalpy during the crystallization processes. After melting composition, the effect of IESF acting as a nucleation agent leads to a quicker crystallization rate of PP during the crystallization process, thus leading to the sharpening of the crystallization peaks and the decreasing crystallization supercooling degrees of the IESF/PP composites. The sharpening of melting peaks and the rising of melting temperatures of the IESF/PP composites should be attributed to the increase of the perfection

TABLE II
The Thermal Parameters of the IESF/PP Composites during the Crystallization and Melting Processes

Sample	T_c (°C)	ΔH_c (J/g)	T_m (°C)	ΔH_m (J/g)
PP	114.6	−76.09	162.0	60.07
IESF/PP	124.2	−71.50	164.1	48.03
IESF/PP/MAPP	125.6	−71.54	164.6	47.06
IESF-SA/PP	125.1	−59.15	164.6	43.16
IESF-NDZ/PP	124.1	−57.24	164.3	31.79

degree of the PP crystallites with less crystalline defects during cooling process due to the nucleation effect of IESF. As for the IESF/PP composites with the same content of PP, the favorable effect of MAPP and SA coupling agents for increasing the crystallization and melting temperatures may imply that the increase of the compatibility (the interactions) between the filler particles and polymer matrix can improve the nucleating activity of the filler.[14] In addition, the greatest values of temperature and enthalpy of IESF/PP/MAPP during the crystallization process, with greater perfection degree and crystallinity of PP crystallites, can be ascribed to the best compatibility between the filler and the polymer matrix formed with the effect of the MAPP coupling agent. Correspondingly, the compatibility between the filler and the polymer matrix plays an important role in the effect of nucleation agent of the filles. It should be also noted that there is a small shoulder peak at 152.0°C during the second heating scan of the PP composites with SA surface treatment. Generally, the appearance of the melting peak at 152.0°C is ascribed to the melting of the β-phase of PP.[15] In fact, the β-phase of PP is not very stable, and is easy to be changed to the α-phase, especially under moderate heat treatment conditions. During the second heating scans of pure PP and other IESF/PP composites, there exists merely one endothermic peak without any shoulder peak, which may imply that the surface treated IESF with SA may have

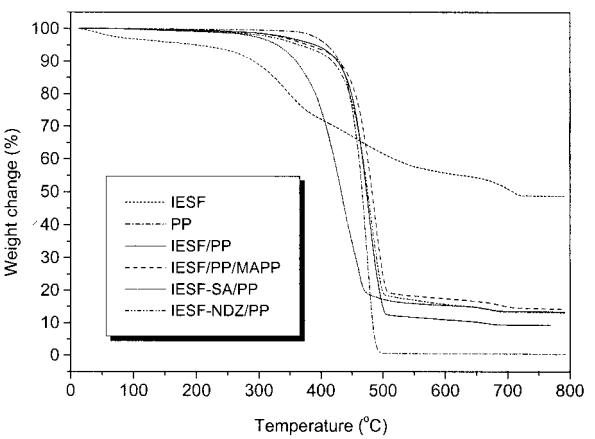

Figure 4 The thermogravimetric analysis of the IESF/PP composites.

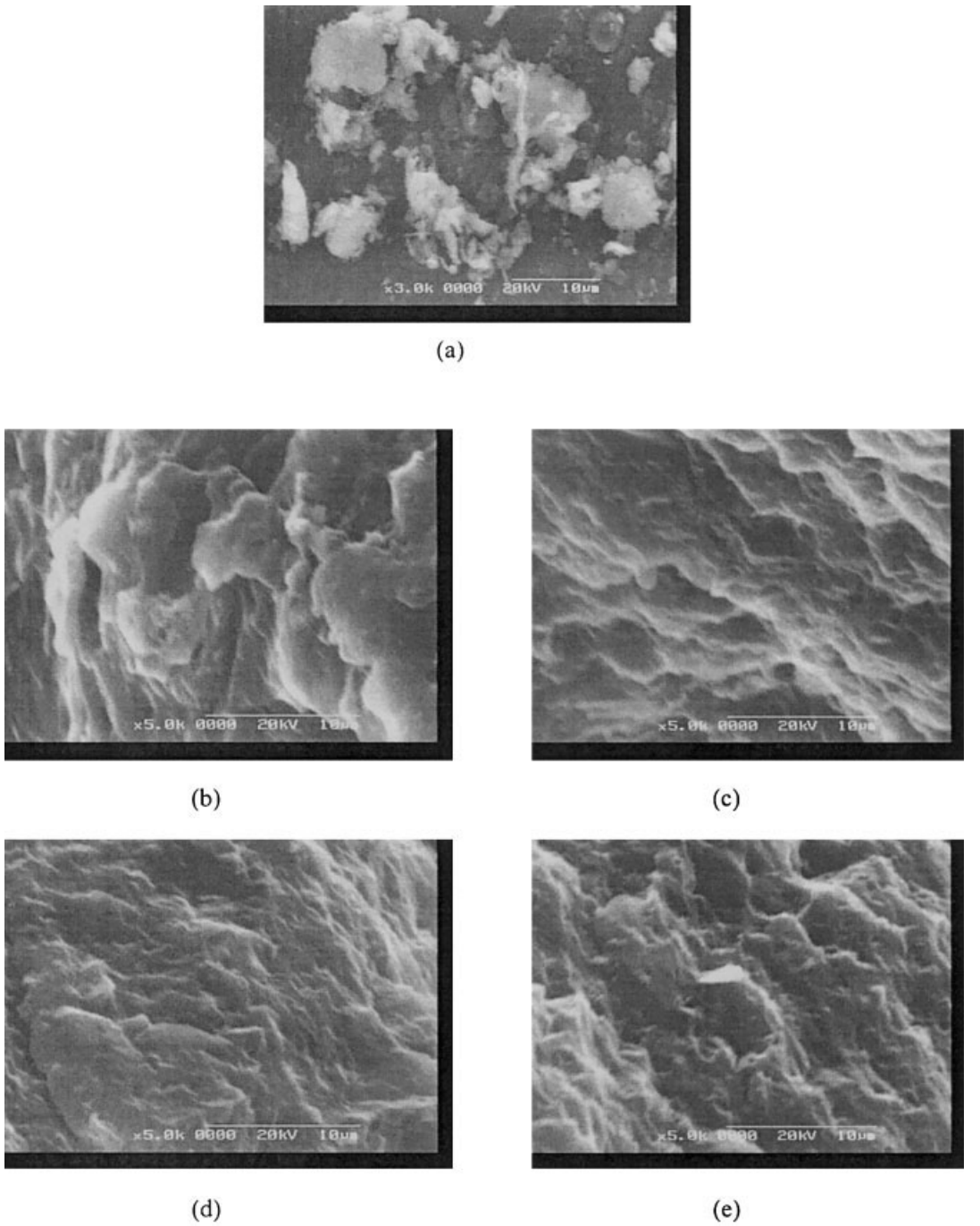

Figure 5 The SEM photographs of IESF and IESF/PP composites: (a) IESF; (b) IESF/PP; (c) IESF/PP/MAPP; (d) IESF-SA/PP; (e) IESF-NDZ/PP.

some beneficial effect on the stabilization of the β-phase of PP.

The thermogravimetric analysis experimental results of the IESF/PP composites are shown in Figure 4. In the light of IESF, the initial weight loss was 4.0% around 100.0°C, the following degradations were at the onset temperatures of 288.6 and 672.9°C with the maximal weight loss values of 39.9 and 6.5%, respectively, and the final ash content was found to be 49.6%. Correspondingly, from the TGA experimental data, it can be concluded that the moisture content of IESF is 4.0%, and the contents of organic and inorganic materials are 46.4 and 49.6%, respectively. From the thermal degradation curves in Figure 4, it can also be found that the initial thermal degradation temperature sequence of these materials can be given as PP > IESF/PP > IESF/PP/MAPP > IESF-NDZ/PP > IESF-SA/PP > IESF, and the maximal and minimal degradation onset temperatures are 448.7 and 381.5°C for PP and IESF-SA/PP separately. In view of this, the

TABLE III
The Mechanical Properties of the IESF/PP Composites

Sample	Izod impact strength (unnotched, J/m)	Izod impact strength (notched, J/m)	Tensile strength (MPa)	Flexural strength (MPa)	Flexural modulus (MPa)	Hardness (N/mm^2)
PP	No break	570.4	26.5	30.2	973.5	53.8
IESF/PP	621.8	44.0	22.8	34.1	1489.0	66.9
IESF/MAPP/PP	475.4	31.4	24.0	35.4	1565.0	66.8
IESF-SA/PP	639.4	41.4	23.0	35.5	1573.7	65.1
IESF-NDZ/PP	512.6	39.4	22.0	34.4	1572.7	65.7

coupling agents have a decreasing influence on the thermal stability of the composite materials, especially SA.

Morphology investigation

SEM is an effective media for the morphology investigations. Through SEM inspection, the distribution of cellulose fiber and inorganic materials and the compatibility between the IESF and the polymer matrix could be observed. The SEM photographs of the IESF and the IESF/PP composites are illustrated in Figure 5. In Figure 5(a), the inorganic particles appear spherical and the short cellulose fibers appear cotton-like with aggregated structure. The formation of aggregates of the fibers should be ascribed to the strong interaction of the hydroxyl groups in the fibers. After blending of IESF with PP, the IESF particles could not be clearly seen in the fracture surface of the PP composites. This phenomenon can further verify that the IESF particles are involved in the coiling molecular chains of PP during the melting processing. When the composites were cooled from the melt, the dispersed IESF particles acted as a nucleation agent and fastened the crystallization of the PP segments. For the composite of IESF/PP, in the presence of the coupling agents, the distribution of the components becomes more uniform and the interface adhesion turns better, indicating the increase in the compatibility between the filler and polymer matrix for the other PP composites. As seen from Figure 5, it seems that the compatilizer effect of MAPP is more obvious than the other two coupling agents. Just as reported before,[2] MAPP not only has a compatilizer effect on the fiber and polymer composites, but also can act as a dispersing agent between polar fillers and unpolar polymer matrix, thus resulting a good dispersion of the fillers. The strong interaction between the hydrophilic filler and the hydrophobic polymer matrix can be attributed to the formation of hydrogen bonds between the hydroxyl groups of fibers and the anhydride groups of MAPP in the interfacial region.

Mechanical properties

The mechanical properties of the IESF/PP composites are given in Table III. It can be observed in Table III that after the IESF filler addition, the decrease of the impact and tensile strength and the increase of the flexural strength occur, and both the decrement of the impact strength and the increment of flexural modulus are great with the values of more than 92 and 53%, respectively. Among the IESF/PP composites, the coupling agents have a slight influence on the mechanical properties, and even cause some decrease in the impact strength. Although MAPP has a favorable compatilizer effect on the interfacial adhesion between the IESF and PP matrix, the original greater rigidity of MAPP over PP may cause some negative effects on the impact property.

It can be inferred from the hardness values in Table III that the IESF/PP composites have higher hardness values than that of PP. In addition, the coupling agent addition makes the hardness decrease slightly, which may be attributed to the increase of the interfacial adhension between the IESF filler and the PP polymer matrix. From the hardness measurements, it can also be found that the composite with the MAPP coupling agent addition is more rigid than the composites with other coupling agent treatments.

Heat distortion temperature measurement reflects the dimensional stability. Just as measured with the HDT/Vicat Softening Point Apparatus, the HDT values were 44.6, 48.9, 48.5, 49.4, and 49.4°C for PP, IESF/PP, IESF/PP/MAPP, IESF-SA/PP, and IESF-NDZ/PP, respectively. Thus, it can be seen that both the IESF filler and the coupling agent addition can have a positive effect on the improvement of dimensional stability.

CONCLUSION

In this article, ink-eliminated sludge flour (IESF) from the recycling treatments of waste paper was utilized as a filler for polypropylene (PP). It was found that the addition of IESF not only induced the crystallization orientation of iPP along the b-axis, but also had a restraining effect on the crystallization of the β-phase of iPP at the same time. In addition, the coupling agent addition can lead to a little increase in the crystallite size of both the α and β crystalline phases of PP. Due to the nucleation agent effect of IESF, the PP composites possess quicker crystallization rate and lower crystallization supercooling degree during the crystal-

lization process. Among the PP composites, the IESF/PP/MAPP composite possesses the greatest values of temperature and enthalpy during the crystallization processes. As for the mechanical properties, after the IESF filler addition, the decrease of the impact and tensile strength and the increase of the flexural strength and the hardness occur, and both the decrement of the impact strength and the increment of flexural modulus are relatively very great. The coupling agent addition has slight influence on the mechanical properties, and even causes some decrease in the impact strength. Both the IESF filler and the coupling agent addition can have a favorable effect on the improvement of dimensional stability, but the coupling agent has a negative effect on the thermal stability of the composites at the same time.

The authors are grateful for the support of the Shanghai Postdoctoral Foundation and sincerely thank the Shanghai Nuo Ya Environmental Resources Exploitation Limited Company for the supply of paper sludge flour.

References

1. Son, J.; Kim, H.-J.; Lee, P.-W. J Appl Polym Sci 2001, 82, 2709.
2. Jang, J.; Lee, E. Polym Test 2001, 20, 7.
3. Oksman, K.; Clemons, C. J Appl Polym Sci 1998, 67, 1503.
4. Ichazo, M. N.; Albano, C.; Gonzalez, J.; Perera, R.; Candal, M. V. Comp Struct 2001, 54, 207.
5. Wu, J. S.; Yu, D. M.; Chan, C.-M.; Kim, J.; Mai, Y.-W. J Appl Polym Sci 2000, 76, 1000.
6. Amash, A.; Zugenmaier, P. Polym Bull 1998, 40, 251.
7. Gassan, J.; Bledzki, A. K. Composites Part A 1997, 28A, 1001.
8. Mi, Y. L.; Chen, X. Y.; Guo, Q. P. J Appl Polym Sci 1997, 64, 1267.
9. Chen, X. Y.; Guo, Q. P.; Mi, X. L. J Appl Polym Sci 1998, 69, 1891.
10. Chuai, C. Z.; Almdal, K.; Poulsen, L.; Plackett, D. J Appl Polym Sci 2001, 80, 2833.
11. Feng, D.; Caulfield, D. F.; Sanadi, A. R. Polym Compos 2001, 22, 506.
12. Alonso, M.; Velasco, J. I.; de Saja, J. A. Eur Polym J 1997, 33, 255.
13. Hsieh, Y. L.; Mo, Z. S. J Appl Polym Sci 1987, 33, 1479.
14. Qiu, W. L.; Mai, K. C.; Zeng, H. M. J Appl Polym Sci 2000, 77, 2974.
15. Jacoby, P.; Bersted, B. H.; Kissel, W. J.; Smith, C. E. J Polym Sci Polym Phys Ed 1986, 24, 461.